

Generalization of the Fedorova-Schmidt method for determining particle size distributions

Salvino Ciccariello

*Università di Padova, Dipartimento di Fisica G. Galilei
Via Marzolo 8, I-35131 Padova, Italy.
E-mail salvino.ciccariello@unipd.it; Phone +39 0473 690808;
Fax +39 049 8277102*

July 21, 2014

Abstract

One reports the integral transform that determines the particle size distribution of a given sample from the small-angle scattering intensity under the assumption that the particle correlation function is a polynomial of degree M . The Fedorova-Schmidt solution [*J. Appl. Cryst.* **11**, 405, (1978)] corresponds to the case $M = 3$. The procedure for obtaining a polynomial approximation to a particle correlation function is discussed and applied to the cases of polydisperse particles of tetrahedral or octahedral or cubical shape.

Synopsis: It is reported the integral transform that determines the particle size distribution from the small angle scattering intensity under the assumption that the particle correlation function is a polynomial.

Keywords: polydisperse samples, size distribution determination, small-angle scattering, polyhedral particles.

1 Introduction

Colloidal suspensions, demixing alloys, porous glasses, carbons are classical examples of materials that have a particulate structure on a length scale of 1-10³nm. For these samples scattering data can successfully be used to determine the particle size distribution in the favorable cases where: a) the constituting particles and the surrounding medium are fairly homogeneous on a spatial resolution of 1nm, b) the sample particles have the same geometrical shape and are isotropically distributed, and c) interference effects among different particles are negligible. The application of this procedure to small-angle scattering (SAS) intensities traces back to the contributions of Roess(1946) and Roess & Shull (1947). In particular, Roess & Shull devised an early scheme whereby the particle size distribution could be found by comparing the observed SAS intensity with plots of theoretical intensities numerically evaluated by considering reasonable particle shape and appropriate size-distribution functions. Besides, Roess (1946) also showed that the size distribution can be expressed as an integral transform of the observed intensity in the case of spherical shape. This interesting result was improved and successfully applied by Letcher & Schmidt(1966) to get the particle size distributions of three Ludox samples by the analysis of their small-angle x-ray (SAXS) intensities. Some years later Fedorova & Schmidt (1978) generalized the previous result showing that the size distribution can be expressed as an integral transform of the SAS intensity for all the particle shapes characterized by an isotropic form factor of the following form

$$\frac{[v \ell^\alpha J_\nu(q\ell)]^2}{(q\ell)^\beta} \quad (1)$$

where $q = (4\pi/\lambda) \sin(\theta/2)$ is the scattering vector (λ denoting the particle beam wave-length and θ the scattering angle), ℓ denotes the maximal chord of the particle, $v \ell^\alpha$ its volume, ν , α and β depend on the particle shape and dimensionality, and $J_\nu(\cdot)$ is the Bessel function of the 1st kind. The shapes allowed by this more general formulation include hollow spheres, disks of negligible thickness and uniform or hollow cylinders of infinite length. Besides, in all these cases, Fedorova and Schmidt worked out the integral transform that yields the size distribution from the SAS intensity collected with the pin hole or the infinite slit geometry.

The main aim of this paper is to get a generalization of this result.

In fact, it will be shown that the size distribution can be written as an integral transform of the collected intensity in all the cases where the particle correlation function is an M degree polynomial $P_M(r)$ continuous, together with its first $m(< M)$ derivatives, throughout $[0, \infty]$. Consider a particle of maximal chord ℓ . The correlation function (CF) of this particle identically vanishes once r exceeds ℓ . Hence, the above assumption of continuity is equivalent to state that the CF and its first m derivatives vanish at $r = \ell$.

The plan of the paper is as follows. For completeness, section 2 reports the expression of the correlation function (CF) in terms of the so-called stick probability functions (Debye *et al.* 1957; Goodisman & Brumberger, 1971) while § 3 expresses the observed scattering intensity in terms of the particle

CF, the particle size distribution and a further contribution related to the overlapping of different particles. The Fourier transform of this contribution, on the average, negatively contributes to the observed scattering intensity and vanishes in the infinite dilution limit. Hence, as firstly pointed out by Guinier and Fournet (1955), the relation exploited by polydisperse analysis is physically consistent only for highly diluted samples. Sections 4 and section 5 respectively report the generalization of the Fedorova-Schmidt result in direct and in reciprocal space. Section 6 first discusses how to construct a polynomial approximation of a particle CF, and then, in §6.1, 6.2.1 and 6.2.2, analyzes the cases of the sphere, the cube/octahedron and the tetrahedron. The final conclusions are reported in §7.

2 Stick probability functions and correlation function

The scattering intensity $I(q)$ is the square modulus of the Fourier transform (FT) of $n(\mathbf{r})$, the scattering density of the sample. In the SAS domain, $n(\mathbf{r})$ is fairly approximated by a two value function that can therefore be written as

$$n(\mathbf{r}) = n_1\rho_1(\mathbf{r}) + n_2\rho_2(\mathbf{r}) \quad (2)$$

where n_1 (n_2) denotes the scattering density of phase 1 (2) and $\rho_1(\mathbf{r})$ defines the full geometry of phase 1 since it is equal to 1 or 0 depending on whether the tip of \mathbf{r} falls inside or outside phase 1. (The definition of $\rho_2(\mathbf{r})$ is quite similar.) The spatial region occupied by the i th phase will be denoted as \mathcal{V}_i and its volume by V_i . The volume of the sample is $V = V_1 + V_2$ and the ratio $\varphi_i \equiv V_i/V$ is the volume fraction of the i th phase. According to Debye *et al.*(1957) the *stick probability function* relevant to the i th and j th phase is defined as

$$P_{i,j}(r) = \frac{1}{4\pi V} \int d\hat{\omega} \int \rho_i(\mathbf{r}_1)\rho_j(\mathbf{r}_1 + r\hat{\omega})dv_1, \quad i, j = 1, 2. \quad (3)$$

Here $\hat{\omega}$ is a unit vector that spans all possible directions. Function $P_{i,j}(r)$ is the angular average of the volume fraction of the overlapping region between phases i and j , once the latter has been translated by $-r\hat{\omega}$. It also represents the probability that a stick of length r , after having been randomly tossed a very large number of times, falls with one end inside phase i and the other end within phase j . The $P_{i,j}(r)$ s have the following properties [Goodisman & Brumberger (1971), Ciccariello *et al.*(1981), Ciccariello (1984)]

$$P_{i,j}(r) = P_{j,i}(r), \quad P_{i,1}(r) + P_{i,2}(r) = \varphi_i, \quad (4)$$

$$P_{i,j}(0) = \varphi_i\delta_{i,j}, \quad P_{i,j}(\infty) = \varphi_i\varphi_j, \quad P'_{i,j}(0) = (-1)^{i+j}S/4V, \quad (5)$$

$$P''_{i,j}(0) = (-1)^{i+j} \sum_j \frac{L_j}{3\pi V} (1 + (\pi - \beta_j) \cot \beta_j), \quad (6)$$

$$P_{i,j}'''(0) = (-1)^{i+j} \frac{1}{16V} \int_S (3H^2(\mathbf{r}) - K_G(\mathbf{r})) dS + \frac{S_{i,j}}{4V}. \quad (7)$$

Here the prime denotes the derivative, S the area of the interphase surface, L_j the length of the j th edge present on the interface, β_j the associated dihedral angle. Further, in (7), $H(\mathbf{r})$ and $K_G(\mathbf{r})$ respectively denote the mean and the Gaussian curvature of the interface at the point \mathbf{r} and $S_{i,j}$ a further contribution that is only present when the interphase surface presents edges meeting at some vertices. We defer to Kirste and Porod (1962) for the derivation of the integral contribution and to Ciccariello & Sobry (1995) for the explicit expression of $S_{i,j}$.

For a statistically isotropic sample one finds that [Debye *et al.*(1957), Goodisman & Brumberger (1971), Ciccariello *et al.*(1981)] the scattering intensity $I(q)$ is

$$I(q) = \frac{4\pi}{q} \langle \eta^2 \rangle V \int_0^\infty r \sin(qr) \Gamma(r) dr \quad (8)$$

with

$$\Gamma(r) \equiv 1 - (n_1 - n_2)^2 P_{1,2}(r) / \langle \eta^2 \rangle, \quad (9)$$

where $\langle \eta^2 \rangle$ is the mean square scattering density fluctuation, *i.e.*

$$\langle \eta^2 \rangle \equiv \sum_{i=1}^2 (n_i - \bar{n})^2 \varphi_i = (n_1 - n_2)^2 \varphi_1 \varphi_2 \quad (10)$$

with $\bar{n} \equiv (n_1 \varphi_1 + n_2 \varphi_2)$. Function $\Gamma(r)$ is commonly referred to as the correlation function of the sample. By equation. (4b) it takes the form

$$\Gamma(r) = \frac{P_{1,1}(r) - \phi_1^2}{\phi_1 \phi_2}, \quad (11)$$

more useful in our later analysis. From (5) and (11) immediately follows that

$$\Gamma(0) = 1, \quad \Gamma(\infty) = 0, \quad \Gamma'(0) = -S/(4V\varphi_1\varphi_2). \quad (12)$$

Similarly, the expressions of $\Gamma''(0)$ and $\Gamma'''(0)$ are also known by Equation.s (6) and (7).

Multiplying $I(q)$ by $4\pi q^2$, integrating over all the positive qs and using Equation. (8) and (12a), one finds the so-called Porod invariant relation

$$\mathcal{Q}_P \equiv \int_0^\infty q^2 I(q) dq = 2\pi^2 V \langle \eta^2 \rangle. \quad (13)$$

3 The scattering intensity in the polydisperse approximation

Consider now the case of a particulate sample where the particles have the same shape and different sizes. The distribution of the particles in the space

is assumed to be statistically isotropic. The phase formed by the particles will be named phase 1. Hence $\rho_1(\mathbf{r})$ becomes equal to

$$\rho_1(\mathbf{r}) = \sum_J \rho_J(\mathbf{r}), \quad (14)$$

where the sum runs over all the particles, labelled by index J and $\rho_J(\mathbf{r})$ denotes now the characteristic function of the J th particle. The substitution of (14) into the $P_{1,1}(r)$ definition [see equation (3)] yields

$$P_{1,1}(r) = \sum_J \frac{V_J \gamma_J(r)}{V} + \mathcal{R}(r), \quad (15)$$

with

$$\mathcal{R}(r) \equiv \sum_{J \neq L} \frac{1}{4\pi V} \int d\hat{\omega} \int \rho_J(\mathbf{r}_1) \rho_L(\mathbf{r}_1 + r\hat{\omega}) dv_1, \quad (16)$$

$$\gamma_J(r) \equiv \frac{1}{4\pi V_J} \int d\hat{\omega} \int \rho_J(\mathbf{r}_1) \rho_J(\mathbf{r}_1 + r\hat{\omega}) dv_1, \quad (17)$$

and V_J denoting the volume of the J th particle. The sum on the right hand side (rhs) of (15) and function $\mathcal{R}(r)$ respectively are the intraparticle and the interparticle contributions to $P_{1,1}(r)$. The last contribution is poorly known. One knows that it and its first derivative vanish as $r \rightarrow 0$ (because the overlapping between two different particles is possible only if r is greater than the lowest of the particle maximal chord values) and that it approaches φ_1^2 as r becomes very large (because the probability that the stick of length r has its ends within phase 1 is equal to φ_1^2).

We elaborate now the intraparticle contribution. To this aim one observes that function $\gamma_J(r)$ is independent on the actual position and orientation of the particle and only depends on the shape (fixed by assumption) and the size of the particle. It is the (isotropic) correlation function of the J th particle. It is equal to zero as r exceeds ℓ_J , the largest chord of the particle, and is equal to one at $r = 0$. Comparing $\gamma_J(r)$ with $\gamma_L(r)$, it results that $\gamma_J(r) = \gamma_L(\ell_L r / \ell_J)$. Then, denoting by $\gamma(r)$ the CF of the *unit* particle, namely the particle having its largest chord equal to the unit length, one has

$$\gamma_J(r) = \gamma(r/\ell_J). \quad (18)$$

The volume of the J th particle is $V_J = v \ell_j^3$ and the first sum on the rhs of (15) becomes

$$\sum_J \frac{V_J \gamma_J(r)}{V} = v \sum_j \frac{N_j \ell_j^3}{V} \gamma(r/\ell_j) = \frac{v N_t}{V} \sum_j \frac{N_j}{N_t} \ell_j^3 \gamma(r/\ell_j), \quad (19)$$

where the sum runs now over the particles' different sizes labelled by j . Moreover, we have denoted by N_j the number of particles with the j th size,

and by N_t the total number of the particles present in the sample. As V becomes infinitely large, N_t/V becomes equal to n , the particle number mean density of the sample and, what is more important, since j runs over a very large number, N_j/N_t can be approximated by the infinitesimal quantity $p(\ell)d\ell$ where $p(\ell)$ represents the probability density of finding a particle of size ℓ within the interval $[\ell, \ell + d\ell]$. Then, the first sum on the rhs of (15) converts into an integral, *i.e.*

$$\sum_J \frac{V_J \gamma_J(r)}{V} \rightarrow v n \int_0^\infty \ell^3 p(\ell) \gamma(r/\ell) d\ell = v n \int_r^\infty \ell^3 p(\ell) \gamma(r/\ell) d\ell. \quad (20)$$

From equations (11) and (15) one finds that the sample CF is the sum of two terms

$$\Gamma(r) = \Gamma_p(r) + \Gamma_i(r), \quad (21)$$

with

$$\Gamma_p(r) \equiv \frac{v n}{\varphi_1 \varphi_2} \int_0^\infty \ell^3 p(\ell) \gamma(r/\ell) d\ell \quad (22)$$

and

$$\Gamma_i(r) \equiv \frac{\mathcal{R}(r) - \varphi_1^2}{\varphi_1 \varphi_2}. \quad (23)$$

The CF's definition requires that $\Gamma(0) = 1$. Setting $r = 0$ into (22) and observing that the particle mean volume \bar{v}_p is given by

$$\bar{v}_p = v \int_0^\infty \ell^3 p(\ell) d\ell \quad (24)$$

so that $\varphi_1 = n \bar{v}_p$, one finds that

$$\Gamma_p(0) = \frac{v n}{\varphi_1 \varphi_2} \int_0^\infty \ell^3 p(\ell) d\ell = \frac{n \bar{v}_p}{\varphi_1 \varphi_2} = \frac{1}{\varphi_2}. \quad (25)$$

Since $\mathcal{R}(0) = 0$, one also finds that

$$\Gamma_i(0) = -\varphi_1/\varphi_2. \quad (26)$$

From (25) and (26) one concludes that neither $\Gamma_p(r)$ nor $\Gamma_i(r)$ are CFs and that the only $\Gamma(r)$ shares this property because $\Gamma(0) = 1$. By Fourier transforming relation (21), multiplied by $\langle \eta^2 \rangle V$, and putting

$$\mathcal{C} \equiv (n_1 - n_2)^2 v n V, \quad (27)$$

one finds that the scattering intensity, given by (8), separates into two contributions, *i.e.*

$$I(q) = I_p(q) + I_i(q) \quad (28)$$

with

$$I_p(q) \equiv \frac{4\pi\mathcal{C}}{q} \int_0^\infty \ell^3 p(\ell) d\ell \int_0^\infty r \sin(qr) \gamma(r/\ell) dr, \quad (29)$$

and

$$I_i(q) \equiv \frac{4\pi\mathcal{C}}{q} \int_0^\infty r \sin(qr) \left(\frac{R(r) - \varphi_1^2}{\varphi_1 \varphi_2} \right) dr. \quad (30)$$

$I_p(q)$ and $I_i(q)$ respectively represent the intraparticle and the interparticle contribution to the scattering intensity. It is noted that Guinier & Fournet (1955) first discussed the importance of the contribution $I_i(q)$, which was mainly analyzed in the molecular approximation. Apply now the basic relation

$$\frac{1}{2\pi^2} \int_0^\infty q^2 dq \left(\frac{4\pi}{q} \int_0^\infty r \sin(qr) f(r) dr \right) = f(0), \quad (31)$$

to $I_p(q)$ and $I_i(q)$. One respectively finds

$$\begin{aligned} \mathcal{Q}_{p,P} &\equiv \int_0^\infty q^2 I_p(q) dq = 2\pi^2 \langle \eta^2 \rangle V \Gamma_p(0) = \\ &\frac{2\pi^2 \langle \eta^2 \rangle V}{\varphi_2} = 2\pi^2 (n_1 - n_2)^2 N_t \bar{v}_p \end{aligned} \quad (32)$$

and

$$\begin{aligned} \mathcal{Q}_{i,P} &\equiv \int_0^\infty q^2 I_i(q) dq = 2\pi^2 \langle \eta^2 \rangle V \Gamma_i(0) = \\ &-\frac{2\pi^2 \langle \eta^2 \rangle V \varphi_1}{\varphi_2} = -2\pi^2 (n_1 - n_2)^2 N_t n \bar{v}_p^2 < 0. \end{aligned} \quad (33)$$

The negativeness of $\mathcal{Q}_{i,P}$ implies that $I_i(q)$ is negative in some q -ranges so that $I_i(q)$ is not a scattering intensity but only a FT. Owing to the fact that $\mathcal{R}'(r)$ also tends to zero as $r \rightarrow 0$, it follows that $I_i(q)$ decreases faster than q^{-4} as $q \rightarrow \infty$. One concludes that the asymptotic behaviour of $I(q)$ is equal to that of $I_p(q)$. The last one immediately follows from (29) and from the fact that $\gamma'(0) = -s/4v$, where s denotes the surface area of the unit particle. One finds that Porod's law (Porod, 1951) takes the form

$$I(q) \approx I_p(q) \approx \frac{2\pi(n_1 - n_2)^2 s N_t}{q^4} \int_0^\infty \ell^2 p(\ell) d\ell = \frac{2\pi(n_1 - n_2)^2 N_t \bar{s}_p}{q^4} = \frac{P_{rd}}{q^4}, \quad (34)$$

with

$$\bar{s}_p \equiv s \int_0^\infty \ell^2 p(\ell) d\ell \quad (35)$$

denoting the particle mean surface area, $\bar{S} \equiv N_t \bar{s}_p$ and $P_{rd} \equiv 2\pi(n_1 - n_2)^2 \bar{S}$. Moreover, the only sum of (32) and (33) yields the correct Porod invariant

[i.e. (13)].

The polydisperse approximation consists in setting $I_p(q) \approx I(q)$ and neglecting $I_i(q)$ (Guinier & Fournet, 1955; Feigin & Svergun, ; Gille, 2013). The approximation is certainly correct at large qs for the behaviour of $I_i(q)$. The last contribution is only appreciable at small qs where the approximation $I_p(q) \approx I(q)$ consequently fails unless the sample is very dilute, because $I_i(q)$ vanishes as $\varphi_1 \rightarrow 0^1$. Only in this case $I_p(q)$ fairly fulfills the Porod invariant relation because the rhs of (32) closely approaches $2\pi^2\langle\eta^2\rangle V$.

Finally, it is observed that the knowledge of $\mathcal{Q}_{p,P}$, P_{rd} and $p(r)$ only determines $(n_1 - n_2)^2 N_t$ since one has $(n_1 - n_2)^2 N_t = \frac{\mathcal{Q}_{p,P}}{2\pi^2\bar{v}_p} = \frac{P_{rd}}{2\pi^2\bar{s}_p}$. From the last equality one obtains that $\frac{\bar{s}_p}{\bar{v}_p} = \frac{P_{rd}}{\mathcal{Q}_{p,P}}$ which tests the accuracy of $p(r)$.

4 Generalization of the Fedorova-Schmidt method

Hereafter it will be assumed that the approximation $I_p(q) \approx I(q)$ holds true and the problem of obtaining an integral transform that directly determines $p(\ell)$ from the scattering intensity $I(q)$ will now be tackled. In principle, if $I(q)$ is known throughout the full q -range, function $G(r)$, defined as

$$G(r) \equiv \frac{1}{2\pi^2 \mathcal{C}} \int_0^\infty q \sin(qr) I(q) dq, \quad (36)$$

also is fully known. On the other hand, by equation (29) one finds that

$$\frac{1}{2\pi^2 \mathcal{C}} \int_0^\infty q \sin(qr) I(q) dq = \int_0^\infty \ell^3 p(\ell) \gamma(r/\ell) d\ell. \quad (37)$$

Combining (36) and (37) and putting, for notational simplicity,

$$\mathcal{P}(\ell) \equiv \ell^3 p(\ell), \quad (38)$$

one gets the integral equation

$$\int_0^\infty \mathcal{P}(\ell) \gamma(r/\ell) d\ell = G(r), \quad (39)$$

¹A heuristic way for overcoming the high dilution assumption consists in assuming that $\mathcal{R}(r)$ has a known parameterized form, for instance $\mathcal{R}(r) = \varphi_1^2(1 - (1 + \mu r)e^{-\mu r} \cos(\nu r))$, which vanishes together with its derivative as $r \rightarrow 0$ and tends to φ_1^2 as $r \rightarrow \infty$. Then $\Gamma_i(r)$ is obtained by (23), $I_i(q)$ by (30) and $I_p(q)$ is known (in terms of μ and ν) by the relation $I_p(q) = I(q) - I_i(q)$. Finally the four relations (13), (32), (33) and (34) in principle determine, $(n_1 - n_2)^2$, N_t , μ and ν .

which, once solved, determines $\mathcal{P}(\ell)$, and hence $p(\ell)$ via (38), in terms of $G(r)$, and hence of $I(q)$ via (36). Using the property that $\gamma(r)$ identically vanishes if $r > 1$, equation (39) converts into

$$G(r) = \int_r^\infty \mathcal{P}(\ell)\gamma(r/\ell)d\ell. \quad (40)$$

Our task now is that of showing that the (integral) transform that expresses $\mathcal{P}(\ell)$ in terms $\gamma(r)$ and $G(r)$ can be explicitly written down if one assumes that:

- *i) $\gamma(r)$ is an M th degree polynomial, i.e.*

$$\gamma(r) = \sum_{i=0}^M a_i r^i, \quad M \geq 3, \quad (41)$$

with $a_0 = 1$ and $a_1 = -s/4v$,

- *ii) $\gamma(r)$ and its first m derivatives (with $1 \leq m < M$) vanish at $r = 1$, i.e. after putting*

$$g_m \equiv \gamma^{(m)}(1) \quad \text{for } m = 0, 1, \dots, M, \quad (42)$$

one assumes that

$$g_0 = g_1 = \dots = g_m = 0, \quad (43)$$

- *iii) $\mathcal{P}(\ell)$ exponentially decreases as $\ell \rightarrow \infty$ and, as $\ell \rightarrow 0$, it goes to zero sufficiently fast for the later considered integrals to exist.*

Owing to assumption *ii*), from (40) follows that

$$G^{(k)}(r) = \int_r^\infty \ell^{-k}\mathcal{P}(\ell)\gamma^{(k)}(r/\ell)d\ell \quad \text{if } 0 \leq k \leq m+1. \quad (44)$$

For the $(m+2)$ th derivative one can no longer use (43) and one finds that

$$G^{(m+2)}(r) = -g_{m+1} \mathcal{P}(r)/r^{m+1} + \int_r^\infty \ell^{-m-2} \mathcal{P}(\ell) \gamma^{(m+2)}(r/\ell) d\ell. \quad (45)$$

Up to the M th order, the successive derivatives have a similar structure. The $(M+1)$ th derivative however will involve no integral contribution because the integrand vanishes owing to assumption *i*). In this way one finds that $\mathcal{P}(r)$ must obey the following linear inhomogeneous differential equation

$$\sum_{k=0}^{(M-m-1)} g_{M-k} \frac{d^k}{dr^k} (\mathcal{P}(r)/r^{M-k}) = -G^{(M+1)}(r). \quad (46)$$

If $m = (M - 1)$ the sum on the left hand side reduces to a single term so that $\mathcal{P}(r)$ is simply determined by

$$\mathcal{P}(r) = -r^{m+1}G^{(M+1)}(r)/g_{m+1}. \quad (47)$$

If $m < (M - 1)$, Equation. (46) is a genuine differential equation of order $M_p \equiv (M - m - 1)$ yielding $\mathcal{P}(r)$ as one of its solutions.

To get $\mathcal{P}(r)$ one must first determine the general integral of the associated homogeneous differential equation

$$\sum_{k=0}^{M_p} g_{M-k} \frac{d^k}{dr^k} (\mathcal{P}(r)/r^{M-k}) = 0, \quad (48)$$

then find a particular integral of (46) and, finally, impose the appropriate boundary conditions.

Looking for a solution of (48) of the form r^α one finds

$$\sum_{k=0}^{M_p} g_{M-k} \frac{d^k r^{\alpha+k-M}}{dr^k} = r^{\alpha-M} \times \quad (49)$$

$$\sum_{k=0}^{M_p} g_{M-k} (\alpha + k - M)(\alpha + k - 1 - M) \dots (\alpha + 1 - M) = 0.$$

Using the descending Pochhammer symbol $(x)_n$, defined as $(x)_n \equiv x(x - 1)(x - 2) \dots (x - n + 1)$ if $n \geq 1$ and $(x)_n \equiv 1$ if $n = 0$, equality (49) becomes

$$\sum_{k=0}^{M_p} g_{M-k} (\alpha + k - M)_k = 0. \quad (50)$$

It is a polynomial equation of degree M_p in unknown α . For simplicity one assumes that the roots $\alpha_1, \dots, \alpha_{M_p}$ are distinct. (The case where some roots coincide will be discussed later.) The general integral of Equation. (48) is

$$Y(r, c_1, \dots, c_{M_p}) \equiv \sum_{k=1}^{M_p} c_k r^{\alpha_k} \quad (51)$$

where c_1, \dots, c_{M_p} are arbitrary constants.

A particular integral of the non-homogeneous differential equation (46) is easily obtained by the Cauchy method [see §39 of Goursat (1959)]. It reads

$$X(r) = - \int_{r_0}^r Y(r, C_1(y), \dots, C_{M_p}(y)) \left(\frac{y^{m+1} G^{(M+1)}(y)}{g_{m+1}} \right) dy \quad (52)$$

where r_0 is an arbitrarily chosen value and functions $C_1(y), \dots, C_{M_P}(y)$ are the solutions of the following system of M_P linear equations

$$\begin{aligned}
Y(y, C_1, \dots, C_{M_P}) &= 0, \\
\frac{\partial Y(y, C_1, \dots, C_{M_P})}{\partial y} &= 0, \\
&\dots = 0, \\
\frac{\partial^{M_P-2} Y(y, C_1, \dots, C_{M_P})}{\partial y^{M_P-2}} &= 0, \\
\frac{\partial^{M_P-1} Y(y, C_1, \dots, C_{M_P})}{\partial y^{M_P-1}} &= 1,
\end{aligned} \tag{53}$$

that reduces to $Y(y, C_1, \dots, C_{M_P}) = 1$ if $M_P = 1$. The $C_i(y)$ s solutions of this system are

$$C_i(y) = \frac{y^{M_P-1-\alpha_i}}{\prod_{j \neq i} (\alpha_i - \alpha_j)}, \quad i = 1, \dots, M_P, \tag{54}$$

and function $Y(r, C_1(y), \dots, C_{M_P}(y))$ reads

$$Y(r, C_1(y), \dots, C_{M_P}(y)) = \sum_{i=1}^{M_P} \frac{y^{M_P-\alpha_i-1} r^{\alpha_i}}{A_i(\alpha)}, \tag{55}$$

where it has been put

$$A_i(\alpha) \equiv \prod_{j \neq i, j=1}^{M_P} (\alpha_i - \alpha_j) \quad \text{if } M_P > 1, \tag{56}$$

and $A_i(\alpha) \equiv 1$ if $M_P = 1$. The proof that function $X(r)$, defined by Equation. (52), is a solution of differential equation (46) and that (55) is a solution of (53) is reported in appendix A.

The general integral of Equation. (46) is $X(r) + Y(r, c_1, \dots, c_{M_P})$ and the sought for particle probability density has the form

$$p(\ell) = \ell^{-3} (Y(\ell, c_1, \dots, c_{M_P}) + X(\ell)).$$

Condition *iii*) is fulfilled if one chooses $r_0 = \infty$ and $c_1 = c_2 = \dots = c_{M_P} = 0$. In this way the sought for integral transform that allows one to obtain the particle size probability density from $G(r)$ is fully determined and reads

$$p(\ell) = \sum_{i=1}^{M_P} \frac{\ell^{\alpha_i-3}}{g_{m+1} A_i(\alpha)} \int_{\ell}^{\infty} y^{M-\alpha_i-1} G^{(M+1)}(y) dy. \tag{57}$$

Finally, the case of degenerate roots can rigorously be dealt with by the procedure described in §3.3 and 3.4 of Bender & Orszag (1978). In practice one can also proceed, more simply, as follows. Let $\alpha_1 = \alpha_2 = \dots = \alpha_r = \alpha$ be a group of r coinciding roots. One removes the degeneracy by the substitutions $\alpha_i \rightarrow (\alpha + (i - 1)\epsilon)$ with $i = 1, \dots, r$ and ϵ equal to a very small number and then apply the described procedure for determining $p(r)$. By continuity the resulting error will be small with ϵ because all the above reported expressions continuously depend on the α_j s. Hereafter one will confine himself to the non degenerate case.

5 The resolvent kernel in reciprocal space

The integral transform that determines $p(r)$ by the observed scattering intensity $I(q)$ is immediately obtained by taking the $(M + 1)$ derivative of the rhs of (36) and substituting the result into (57). The result is

$$p(r) = \sum_{i=1}^{M_P} \frac{r^{\alpha_i-3}}{2\pi^2 \mathcal{C} g_{m+1} A_i(\alpha)} \int_r^\infty y^{M-\alpha_i-1} \left[D_y^{M+1} \int_0^\infty q \sin(qy) I(q) dq \right] dy, \quad (58)$$

where D_y denotes the derivative operator with respect to y . This result generalizes the Fedorova Schmidt formula because it applies to any CF that has a polynomial form as it happens in the case of spheres. It is noted that the reconstruction of $p(r)$ from the observed intensity, under the assumption of a polynomial CF, holds also true in the case of the slit collimation thanks to Guinier's integral transform (Guinier, 1946) that converts $J(q)$, the intensity collected with the slit geometry, into the pin-hole $I(q)$.

Our task now is that of rewriting (58) in a more compact form that is more convenient for numerical evaluation. To this aim one formally exchanges the integration order in (58) and, after putting

$$K(r, q, \alpha, M) \equiv \int_r^\infty y^{M-\alpha-1} \left[D_y^{M+1} \frac{\sin(qy)}{y} \right] dy, \quad (59)$$

one gets

$$p(r) = \sum_{i=1}^{M_P} \frac{r^{\alpha_i-3}}{2\pi^2 \mathcal{C} g_{m+1} A_i(\alpha)} \int_0^\infty q I(q) K(r, q, \alpha_i, M) dq. \quad (60)$$

It is noted that definition (59) does not always lead to an existing $K(r, q, \alpha, M)$ because, according to Riemann's theorem (Bender & Orszag, 1978), the integral exists only if $M - 2 - \alpha < 0$, a condition that is not *a priori* ensured. However each integral contributing to equation (57) exists owing to assumption *iii*). Consequently the convergence difficulty of (59) is related to the fact that the integration order cannot be exchanged for the α_i s such that $\alpha_i < (M - 2)$. Hence one must handle the case $\alpha_i > (M - 2)$ differently from that where $\alpha_i < (M - 2)$. This will be respectively done in the following two subsections.

5.1 The case $\alpha_i > (M - 2)$

Assume, for simplicity, that all the α_i s are greater than $(M - 2)$. In this case the order of integration is not important and the corresponding $K(r, q, \alpha_i, M)$ s do exist. These can be expressed in terms of some known transcendental functions proceeding as follows. Perform the integration variable change $y \rightarrow rt$ in (59) and momentarily omit index i for notational simplicity. One gets

$$K(r, q, \alpha, M) = r^{-\alpha-2} \int_1^\infty t^{M-\alpha-1} \frac{d^{M+1}}{dt^{M+1}} \left(\frac{\sin(qrt)}{t} \right) dt. \quad (61)$$

Putting $Q_r \equiv qr$, using the identity [Luke, § 2.9, (1969)]

$$\frac{d^m (\sin(qy)/y)}{dy^m} = \frac{q^{m+1}}{y^{m+1}} \frac{d^m (\sin(qy)/q)}{dq^m}, \quad m = 0, 1, 2, \dots, \quad (62)$$

and denoting the derivation operator with respect to Q_r by D_{Q_r} , the previous integral becomes

$$r^{-\alpha-2} Q_r^{M+2} D_{Q_r}^{M+1} \int_1^\infty t^{-\alpha-3} \frac{\sin(Q_r t)}{Q_r} dt.$$

Recalling the definition of $S(x, a)$, the generalized Fresnel sine integral (equation (6.5.8) of Abramowitz & Stegun, 1970), one finds that

$$\kappa_A(Q_r, \alpha) \equiv \int_1^\infty t^{-\alpha-3} \frac{\sin(Q_r t)}{Q_r} dt = Q_r^{\alpha+1} S(Q_r, -2 - \alpha), \quad (63)$$

which can also be expressed in terms of the hypergeometric function ${}_1F_2(a; b, c; x)$ (Luke, 1969) as

$$\kappa_A(Q_r, \alpha) = Q_r^{1+\alpha} \Gamma(-2 - \alpha) \sin \frac{\pi\alpha}{2} + \frac{1}{1+\alpha} {}_1F_2 \left(-\frac{1+\alpha}{2}; \frac{3}{2}, \frac{1-\alpha}{2}; -\frac{Q_r^2}{4} \right). \quad (64)$$

Combining equations (60), (61), (62) and (63) one finds

$$p(r) = \frac{r^{-5}}{2\pi^2 \mathcal{C} g_{m+1}} \int_0^\infty q I(q) \mathcal{K}_A(qr) dq \quad (65)$$

with

$$\mathcal{K}_A(Q_r) \equiv Q_r^{M+2} D_{Q_r}^{M+1} \sum_{i=1}^{M_P} \frac{1}{A_i(\alpha)} \kappa_A(Q_r, \alpha_i). \quad (66)$$

For later convenience it is also mentioned that the leading asymptotic expansion of $\kappa_A(q, \alpha)$ at large Q_r s is

$$\begin{aligned} \kappa_A(Q_r, \alpha) \approx & \frac{\cos Q_r}{Q_r^2} \left(1 - \frac{12 + 7\alpha}{Q_r^2} + \dots \right) + \\ & \frac{\sin Q_r}{Q_r^3} \left(3 + \alpha - \alpha \frac{47 + 12\alpha + \alpha^2}{Q_r^2} + \dots \right). \end{aligned} \quad (67)$$

5.2 The case $\alpha_i < (M - 2)$

One assumes that all the α_i s are smaller than $(M - 2)$. In this case, as it was already said, the convergence at ∞ of each integral present in (57) is ensured by the sufficiently fast decrease of $G^{(M+1)}(y)$. Hence, one writes

$$\int_r^\infty y^{M-\alpha_i-1} G^{(M+1)}(y) dy = \hat{\mathcal{G}}_i - \int_0^r y^{M-\alpha_i-1} G^{(M+1)}(y) dy \quad (68)$$

with

$$\hat{\mathcal{G}}_i \equiv \lim_{r \rightarrow 0} \int_r^\infty y^{M-\alpha_i-1} G^{(M+1)}(y) dy. \quad (69)$$

Owing to condition *iii*), the limit of $p(r)$ as $r \rightarrow 0$ cannot be divergent. Then, from equation (57), it follows that $\hat{\mathcal{G}}_i = 0$ whatever i . Expressing $G^{(M+1)}(y)$ in terms of its FT and omitting index i for simplicity, one finds

$$-\int_0^r y^{M-\alpha-1} G^{(M+1)}(y) dy = -\int_0^r dy \int_0^\infty q dq y^{M-\alpha-1} \frac{D_y^{(M+1)}}{2\pi^2 q \mathcal{C}} \left(\frac{\sin(qy)}{y} \right) I(q).$$

The order of integration can now be exchanged. Using again identity (62) the last integral becomes

$$\frac{1}{2\pi^2 q \mathcal{C}} \int_0^\infty q I(q) dq \left(-\int_0^r dy y^{-\alpha-3} q^{M+2} D_q^{(M+1)} \left(\frac{\sin(qy)}{q} \right) \right). \quad (70)$$

A further change of the integration variable converts the above y -integral into

$$r^{-\alpha-2} Q_r^{M+2} D_{Q_r}^{(M+1)} \left(-\int_0^1 t^{-\alpha-3} \left(\frac{\sin(Q_r t)}{Q_r} \right) dt \right). \quad (71)$$

This integral also can be expressed in terms of an ${}_1F_2(\cdot)$ hypergeometric function, since

$$\begin{aligned} \kappa_B(Q_r, \alpha) &\equiv -\int_0^1 t^{-\alpha-3} \left(\frac{\sin(Q_r t)}{Q_r} \right) dt = \\ &\frac{1}{1+\alpha} {}_1F_2 \left(-\frac{1+\alpha}{2}; \frac{3}{2}, \frac{1-\alpha}{2}; -\frac{Q_r^2}{4} \right), \end{aligned} \quad (72)$$

i.e. the opposite of the hypergeometric contribution present in the rhs of (64). It follows that, at large Q_r , the leading asymptotic term of $\kappa_B(Q_r, \alpha)$ is the opposite of that of $\kappa_A(Q_r, \alpha)$ [see (67)] plus $Q_r^{1+\alpha} \Gamma(-2-\alpha) \sin \frac{\pi\alpha}{2}$. Combining equations (68)-(72) and substituting the result in (58) one finds that

$$p(r) = \frac{r^{-5}}{2\pi^2 \mathcal{C} g_{m+1}} \int_0^\infty q I(q) \mathcal{K}_B(qr) dq \quad (73)$$

with

$$\mathcal{K}_B(Q_r) \equiv Q_r^{M+2} D_{Q_r}^{M+1} \sum_{i=1}^{M_P} \frac{1}{A_i(\alpha)} \kappa_B(Q_r, \alpha_i). \quad (74)$$

5.3 The general case of some α_i s smaller and the others greater than $M - 2$

The expression of the integral transform that determines the particle size distribution from the scattering intensity, whatever the α_i values, immediately follows from (66) and (74). It is

$$p(r) = \frac{r^{-5}}{2\pi^2 \mathcal{C} g_{m+1}} \int_0^\infty q I(q) \mathcal{K}_G(qr) dq \quad (75)$$

with

$$\mathcal{K}_G(Q_r) \equiv Q_r^{M+2} D_{Q_r}^{M+1} \left[\sum_{i=1}^{M_P} ' \frac{1}{A_i(\alpha)} \kappa_A(Q_r, \alpha_i) + \sum_{i=1}^{M_P} '' \frac{1}{A_i(\alpha)} \kappa_B(Q_r, \alpha_i) \right], \quad (76)$$

where the ' and the '' respectively denote that the corresponding sums are restricted to α_i s greater and smaller than $(M - 2)$, and $Q_r = qr$.

Owing to assumption *iii*) the behaviour of the general resolvent kernel $\mathcal{K}_G(qr)$ is such as to ensure the convergence of (75) even though the property does not apply to each term of the sums. Further, the convergence is rather weak as it will appear clear from the discussions reported in the following section.

6 Polynomial approximation of the CF

At this point one wonders: besides the spherical shape, do exist other particle shapes that have a polynomial CF? As yet the answer is unknown. But this does not imply that one cannot use the above finding to approximate the CF of particles with a given shape by a polynomial. To construct such approximations one first recalls that $\gamma(r)$, the CF of a unit particle with a given shape, obeys some general constraints. The simplest of these are:

- a) $\gamma(0) = 1$,
- b) $\gamma'(0) = \sigma$ with $\sigma \equiv -s/4v$ (σ will be hereafter referred to as *specific surface*),
- c) $\gamma(1) = 0$,
- d) $\gamma'(1) = 0$,
- e) $4\pi \int_0^\infty r^2 \gamma(r) dr = V$,
- f) $4\pi \int_0^\infty r^4 \gamma(r) dr = 2VR_G^2$ where R_G denotes the Guinier gyration radius of the particle,

- *g*) $\gamma''(0) = \mathcal{A}$ where \mathcal{A} is the particle *angularity* defined by equation (6) (Porod, 1967; Méring and Tchoubar, 1968; Ciccariello *et al.*; 1981), and
- *h*) $\gamma'''(0) = \mathcal{K}$ where \mathcal{K} , defined by equation (7), is the particle *curvosity* (Kirste & Porod. 1962; Ciccariello & Sobry, 1995).

Besides the listed constraints one might consider other ones. For instance, if the particle shape is such that one does not have a parallelism condition between finite area subsets of the particle surface at a relative distance equal to the particle maximal chord, one also has $\gamma''(1) = 0$. Similarly, *e*) and *f*) are particular cases of the general relation

$$\mathcal{G}_{2m} \equiv 4\pi \int_0^\infty r^{2m} r^2 \gamma(r) dr = V \sum'_{0 \leq h, k, l \leq m} \frac{m! a_l}{h! k! l!} \times \langle R^{2h+l} \rangle \langle R^{2k+l} \rangle, \quad m = 0, 1, 2, \dots \quad (77)$$

that connects the $2m$ th moment of the particle CF to the higher order gyration radii of the particle (see Appendix B for the proof of (77) and for the explanation of the symbols there involved).

According to Shannon's theorem the information content of any SAS intensity is not particularly rich so that a ten of parameters only can be determined (Moore, 1980; and Taupin & Luzzati, 1982). Thus, in performing a polidisperse analysis of the SAS intensity of a given sample, it appears sensible to approximate the particle CF by a polynomial that fulfills some of the above constraints.

In this paper the simplest cases of the third [$P_3(r)$] and fourth [$P_4(r)$] degree polynomial approximations will be considered. In particular, it will be required that the polynomial approximation obeys *a*), *b*), *c*) and *d*) that explicitly accounts for the support properties of the CF, the normalization at $r = 0$ and a single geometrical feature of the particle, namely its specific surface σ . For the 3rd degree case one finds that

$$\gamma(r) \approx P_3(r) = 1 + \sigma r - (3 + 2\sigma)r^2 + (2 + \sigma)r^3. \quad (78)$$

The associated angularity, curvosity, volume and Guinier gyration radius respectively are

$$\begin{aligned} \mathcal{A} &= -(3 + 2\sigma), & \mathcal{K} &= 6(2 + \sigma), \\ V &= \pi(4 + \sigma)/15, & R_G^2 &= (18 + 5\sigma)/(28(4 + \sigma)). \end{aligned} \quad (79)$$

From (78) follows that the g_m coefficients, defined by (42), are

$$g_0 = g_1 = 0, \quad g_2 = g_2(\sigma) = 2(3 + \sigma), \quad g_3 = g_3(\sigma) = 6(2 + \sigma). \quad (80)$$

One clearly has $M = 3$, $m = 1$, $M_p = 1$ and the solution of polynomial equation (50) is

$$\alpha = \alpha(\sigma) = -\sigma/(3 + \sigma). \quad (81)$$

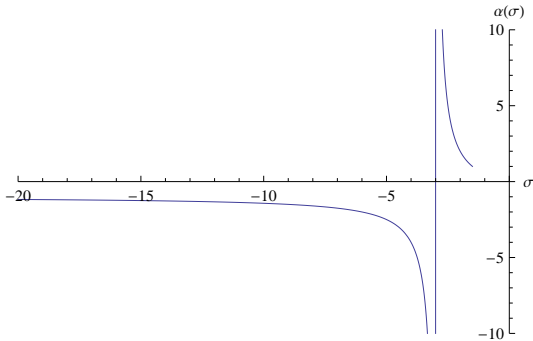


Figure 1: Behaviour of the root of Equation. (50) in terms of the specific surface parameter σ when one considers the 3rd degree polynomial approximation of the particle CF.

Figure 1 plots $\alpha(\sigma)$ vs. σ . It is recalled that σ must be such that $\sigma < -3/2$ because, at fixed volume, the sphere is the geometric solid that has the smallest surface. Thus, α varies between $-\infty$ and ∞ and the variation is very sharp around $\sigma = -3$.

In the following subsections we shall analyze the case of the sphere, that of the cube and the octahedron, that of the tetrahedron and, finally, that of the 4th degree approximation.

6.1 The sphere case

This case, already fully exploited, is mainly reported in order to make fully evident that equations (75) and (76) coincide with those of Fedorova and Schmidt. As it was just said the specific surface of the sphere is $\sigma = -3/2$. The substitution of this value in (78) reproduces the exact CF of the unit sphere, *i.e.*

$$\gamma_{sph}(r) = 1 - 3r/2 + r^2/4. \quad (82)$$

This nice property implies that the constraints relevant to the angularity, the curvosity and all the Guinier higher order gyration radii [see (79)] are exactly obeyed.

As already anticipated it is now shown that integral transform (57) coincides with Fedorova and Schmidt's one in the case of spherical particles. From Eqs. (80) and (81) it follows that $g_2 = 3$ and $\alpha = 1$. Hence Equation. (57) reads

$$p(r) = \frac{1}{3r^2} \int_r^\infty y G^{(4)}(y) dy. \quad (83)$$

Integrating twice by parts, one obtains

$$p(r) = \frac{1}{3r^2} (-rG^{(3)}(r) + G^{(2)}(r)) = -\frac{1}{3} \frac{d}{dr} \left(\frac{G^{(2)}(r)}{r} \right), \quad (84)$$

that coincides with the result of Letcher and Schmidt (1966) and Fedorova & Schmidt (1978).

It is instructive to check equations (57) and (58) choosing as size probability density the (n, λ) Poisson one, namely

$$p(n, \lambda, r) \equiv r^n e^{-\lambda r} / n!, \quad (85)$$

with $n = 4$ and $\lambda = 1$. In the sphere case, the explicit evaluation of (37) yields

$$G(r) = e^{-r} (1680 + 1320r + 480r^2 + 104r^3 + 14r^4 + r^5) / 8. \quad (86)$$

Substituting this expression in the rhs of (84) one straightforwardly verifies that the result coincides with $p(4, 1, r)$.

The check of (58) is more interesting. Since $\alpha = 1$, the size distribution is determined by (65) and (66). The resolvent kernel $\mathcal{K}_A(qr)$, now denoted as $\mathcal{K}_{sph}(qr)$, is

$$\mathcal{K}_{sph}(qr) = (qr)^3 \kappa_{sph}(qr), \quad (87)$$

with

$$\kappa_{sph}(qr) \equiv \cos(qr) \left[1 - \frac{8}{(qr)^2} \right] - 4 \frac{\sin(qr)}{qr} \left[1 - \frac{2}{(qr)^2} \right] \quad (88)$$

and (65) becomes

$$p(r) = \frac{1}{6 \pi^2 \mathcal{C} r^2} \int_0^\infty q^4 I(q) \kappa_{sph}(qr) dq. \quad (89)$$

Function $\kappa_{sph}(qr)$ is such that the integral $\int_0^{\mathcal{Q}_M} \kappa_{sph}(qr) dq$ can be set equal to zero as $\mathcal{Q}_M \rightarrow \infty$ because at large \mathcal{Q}_M it behaves as $\sin(\mathcal{Q}_M r)/r$ that, it being wildly oscillating if $r \neq 0$, averages to zero. Hence, equation (89) can be written in the well known form

$$p(r) = \frac{1}{6 \pi^2 \mathcal{C} r^2} \int_0^\infty (q^4 I(q) - P_{rd}) \kappa_{sph}(qr) dq, \quad (90)$$

which converges faster than (89) at $q = \infty$. Its correctness can explicitly be checked in the case of a (4,1) Poisson distributed spherical particles. The explicit form $I_{p,sph}(q)$ of $I(q)$ is obtained by (29) and reads

$$I_{p,sph}(q) = 24 \mathcal{C} \frac{1050 + 420q^2 + 567q^4 + 329q^6 + 107q^8 + 15q^{10}}{(1 + q^2)^7}. \quad (91)$$

From this expression one finds that $P_{rd} = 360 \mathcal{C}$. Substituting these expressions in the rhs of (90) and evaluating the integral one correctly finds function $p(4, 1, r)$. It is stressed that (90) numerically is much more convenient than (58) to get $p(r)$ from the observed scattering intensity. [A more convenient form has been recently discussed by Botet & Cabane (2012).] Finally, figure 2 shows the size distribution obtained by the numerical evaluation of (90) using as $I(q)$ the values resulting from the numerical integration of (29) in the sphere case (with $\mathcal{C} = 1$).

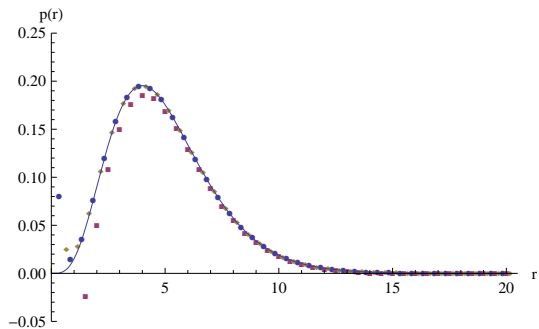


Figure 2: The thin curve plots the (4,1) Poisson distribution. The magenta full squares are the values obtained by Equation. (90) and a numerical evaluation of (29) performed as explained at the end of § 6.2. The blue full circles and the golden diamonds respectively are the values of $p(r)$ reconstructed in the octahedron/cube by (99) and in the tetrahedron case by (102) (see the end of § 6.2).

6.2 The 3rd degree polynomial approximation of the cube's, octahedron's and tetrahedron's CFs

Ciccariello and Sobry (1995) showed that the CF of any polyhedral particle is a 3rd degree polynomial in the innermost r -range. This condition clearly is obeyed by the known CFs of the regular tetrahedron, octahedron (Ciccariello, 2014) and cube (Goodisman, 1980). In these cases the innermost r -range is larger than half the total r -range where the CFs differ from zero. For this reason it is tempting to approximate the known CFs by a 3rd degree polynomial, vanishing together with its first derivative at the outermost r value and subsequently perform a polidisperse analysis along the lines expounded in 6.1. The results of this approximation will now be illustrated. One knows that the specific surface values of the unit cube, the unit octahedron and the unit tetrahedron are respectively equal to

$$\sigma_C = -3\sqrt{3}/2, \quad \sigma_O = -3\sqrt{3}/2, \quad \text{and} \quad \sigma_T = -3\sqrt{3}/2. \quad (92)$$

The 3rd degree polynomial approximations of the three CF immediately result from the substitution of the above σ values into (78). Since the σ values of the cube and the octahedron coincide the resulting 3rd degree approximation of the cube CF is equal to that of the octahedron.

Figure 3 plots the exact CFs and their 3rd degree approximations as well as the FTs of the exact and the polynomial approximated CFs. In direct space the agreement is relatively good for the tetrahedron, reasonable for the cube and not bad for the octahedron since small discrepancies are only present in the outermost r -range. These discrepancies are responsible for those observed at small q 's in reciprocal space. They can be reduced requiring that the polynomial approximations also obey constraint e) because the fulfillment of this constraint implies that the FTs of the exact and the polynomial

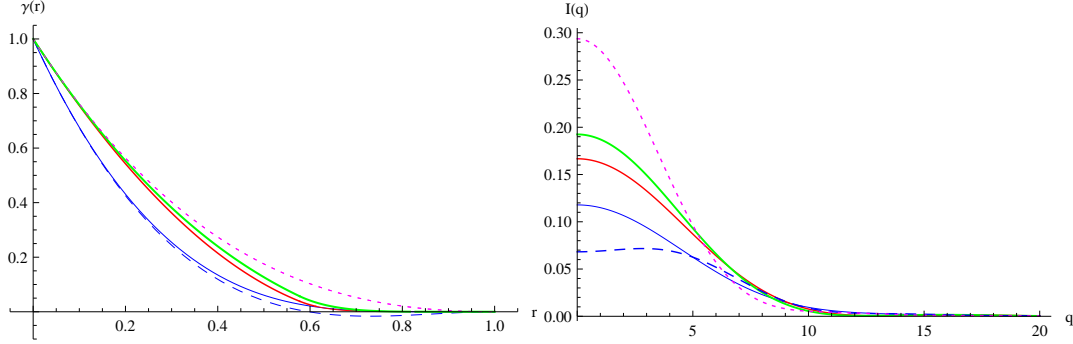


Figure 3: Left: Comparison of the exact CFs with those obtained by the 3rd degree polynomial approximations described in the text. The continuous and broken blue curves refer to the exact and the polynomial approximation of the tetrahedron CF. The continuous red and green ones to the exact CFs of the octahedron and the cube while the dotted magenta curve plots their 3rd degree approximation. Right: Behaviour of the FTs of the CFs shown in the left panel. The symbols are the same.

approximated CFs coincide at $q = 0$. To do that one must consider a 4th degree polynomial approximation, a case discussed in §6.3.

We shall go on with the discussion of the 3rd degree polynomial approximation in the cases of the (4,1) Poisson distributions of cubes, octahedra or tetrahedra. in order to make clear all the point of the analysis.

By Equation. (78) one finds that function $G(r)$, defined by Equation. (40), becomes

$$G_3(r, \sigma) = e^{-r} [210 + 30r(7 + \sigma) + 10r^2(9 + 2\sigma) + 2r^3(11 + 3\sigma) + r^4(13 + 4\sigma)/4 + r^5(3 + \sigma)/12]. \quad (93)$$

Its 3D FT, multiplied by \mathcal{C} , yields the polidisperse scattering intensity, *i.e.*

$$I_3(q, \sigma) = \frac{48\pi \mathcal{C}}{(1 + q^2)^7} [210(4 + \sigma) - 60q^2(1 + 3\sigma) + 7q^4(12 - 19\sigma) + 7q^6(4 - 13\sigma) + q^8(4 - 13\sigma) - 5q^{10}\sigma]. \quad (94)$$

Substituting in the above two relations the σ values reported in Equation.(92) one obtains the CFs as well as the scattering intensities relevant to the three collections of $p(4, 1, d)$ Poisson polidisperse tetrahedrons, octahedrons and cubes. The corresponding exact values are obtained, using the exact particle CFs, by a numerical evaluation of integrals (40) and (29), which can more conveniently be evaluated by

$$I_p(q) = \int_1^\infty y^3 \gamma(1/y) \tilde{p}(4, 1, q, y) dy, \quad (95)$$

with

$$\tilde{p}(4, 1, q, y) \equiv \frac{4\pi}{q} \int_0^\infty r^5 \sin(qr) p(4, 1, r, y) dr = \quad (96)$$

$$\frac{3\pi(8!) q y^5 (5q^4 - 10q^2 y^2 + y^4)(q^4 - 10q^2 y^2 + 5y^4)}{(q^2 + y^2)^{10}}.$$

The results are shown in Figure. 4. The left panel shows the $G(r)$'s and

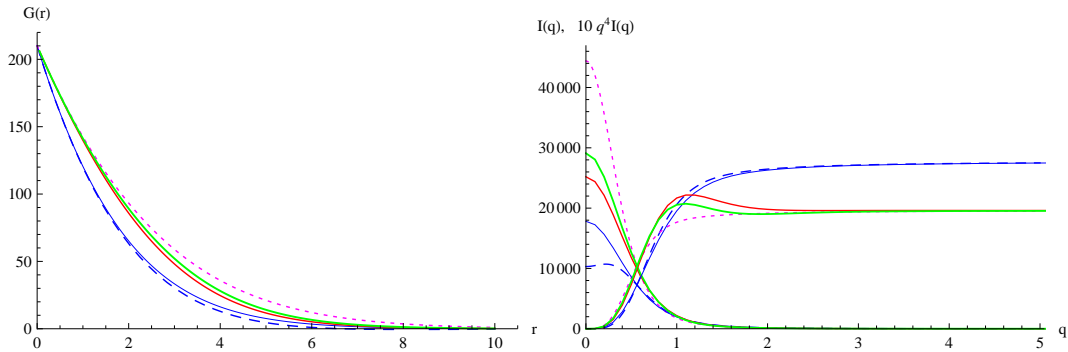


Figure 4: Using the same conventions of Fig. 3, the left panel shows the exact (continuous curves) and the approximated (broken curves) CFs relevant to the (4,1) Poisson polydisperse samples of tetrahedra, octahedra and cubes. The right panel shows the intensities as well as their Porod plots.

the right one the intensities and their Porod plots. For the intensities, the quality of the agreement is similar to that shown in Fig. 3. However, the Porod plots show that the intensity discrepancies observed near the origin are washed out by the factor q^4 . Some discrepancies are still observed around $q = 1$ in the only cubic and octahedral cases, while the agreement is quite satisfactory in the tetrahedron case.

6.2.1 Determination of the size distribution from the scattering intensity in the cube/octahedron case

The root of the resolvent equation relevant to the 3rd degree polynomial approximation of a particle CF is given by equation (81). Since the specific surfaces of the unit octahedron and the unit cube coincide it follows that α is the same in the two case. It will be denoted by $\alpha_{o/c}$. Recalling that σ is equal to $\sigma_{o/c} \equiv -3^{3/2}/2$ [see (92)], one finds

$$\alpha_{o/c} \equiv \alpha(\sigma_{o/c}) = 3 + 2\sqrt{3} \approx 6.46. \quad (97)$$

The resolvent kernel (66) takes now the form $\mathcal{K}_{o/c}(qr) = (qr)^3 \kappa_{o/c}(qr)$, with

$$\begin{aligned} \kappa_{c/o}(Q_r) \equiv & \left(1 - \frac{12 - 5\alpha_{o/c} + \alpha_{o/c}^2}{Q_r^2}\right) \cos Q_r + \left(\alpha_{o/c} - 5 + \right. & (98) \\ & \left. \frac{12 - 7\alpha_{o/c} + 4\alpha_{o/c}^2 - \alpha_{o/c}^3}{Q_r^2}\right) \frac{\sin Q_r}{Q_r} + \alpha_{o/c}^3 \sin \frac{\pi \alpha_{o/c}}{2} \times \\ & (\alpha_{o/c} - 2)\Gamma(-2 - \alpha_{o/c}) + \frac{\alpha_{o/c}}{Q_r^2}(2 - 3\alpha_{o/c} + \alpha_{o/c}^2) \times \\ & {}_1F_2\left(-\frac{1 + \alpha_{o/c}}{2}; \frac{3}{2}, \frac{1 - \alpha_{o/c}}{2}; -\frac{Q_r^2}{4}\right), \end{aligned}$$

and $Q_r = qr$. Also in this case one finds that $\int_0^\infty \kappa_{c/o}(qr) dq = 0$ in the sense reported just below (89), so that (65) can be written as

$$p(r) = \frac{1}{2\pi^2 \mathcal{C} g_2 r^2} \int_0^\infty (q^4 I(q) - P_{rd}) \kappa_{o/c}(qr) dq \quad (99)$$

that is more convenient for numerical computation because the integrand behaves as $const \times \sin(qr)/q$ at large qs .

The result (99) has been analytically checked substituting, in its rhs, $I(q)$ with $I_3(q, s_{o/c})$ given by expression (94) and setting $P_{rd} = \lim_{q \rightarrow \infty} I_3(q, s_{o/c})$. The result is the outset Poisson (4,1) size distribution.

6.2.2 Determination of the size distribution from the scattering intensity in the tetrahedron case

The specific surface of the tetrahedron is given by (92c). Then the root of the resolvent equation associated to the polidisperse polynomial approximation of tetrahedrons is given by (81) and reads

$$\alpha_t \equiv \alpha(\sigma_T) = -3 - \sqrt{6} \approx -5.45. \quad (100)$$

It is smaller than one and therefore one must apply the results of §5.2. The resolvent kernel, defined by (74), is $\mathcal{K}_t(qr) = (qr)^3 \kappa_t(qr)$ with

$$\begin{aligned} \kappa_t(qr) \equiv & \cos(qr) \left(1 - \frac{12 - 5\alpha_t + \alpha_t^2}{q^2 r^2}\right) - & (101) \\ & \frac{\sin(qr)}{qr} \left(5 - \alpha_t - \frac{12 - 7\alpha_t + 4\alpha_t^2 - \alpha_t^3}{q^2 r^2}\right) + \\ & + \frac{\alpha_t (2 - 3\alpha_t + \alpha_t^2)}{q^2 r^2} {}_1F_2\left(-\frac{1 + \alpha_t}{2}; \frac{3}{2}, \frac{1 - \alpha_t}{2}; -\frac{q^2 r^2}{4}\right). \end{aligned}$$

$\kappa_t(qr)$ also is such that $\int_0^\infty \kappa_r(qr) dq = 0$ in the weak sense. One concludes that the particle size distribution in the tetrahedron polynomial approximation is given by

$$p(r) = \frac{1}{2\pi^2 \mathcal{C} g_2 r^2} \int_0^\infty (q^4 I(q) - P_{rd}) \kappa_t(qr) dq. \quad (102)$$

The analytic check of this relation is fully satisfactory as for the case of equation (99) .

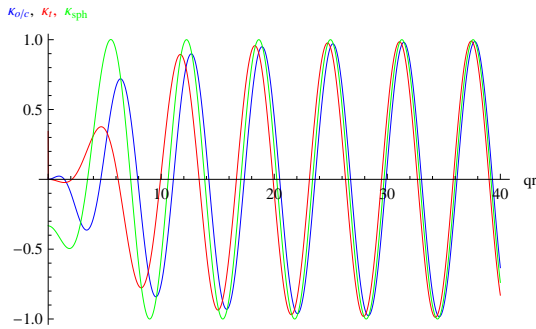


Figure 5: Plots of the resolvent kernels relevant to the sphere case [equation (88), green curve], to the cube/octahedron case [equation (98), blue curve] and to tetrahedron case [equation (101), red curve].

As in the case of Fig. 2, equations (99) and (102) have also been numerically checked as follows. First one evaluates the scattering intensity, given by equation (94), for the octahedron/cube and the tetrahedron cases on a grid of 1000 points uniformly covering the interval $0 < q < 50$. Then one evaluates integrals (98) and (101) using an r -grid of 40 values uniformly distributed over the interval $[0, 20]$. The resolvent kernels (including the sphere case) are plotted in figure 5 and the resulting size distributions are shown in Fig. 2. The agreement is quite satisfactory since the discrepancies observed at small r s are related to the q truncation. For a general discussion of this point see Pedersen (1994).

The $p(r)$ s have also been reconstructed, along the lines just reported, using as scattering intensities those obtained by the exact particle CFs, *i.e.* using equations (95) and (96). The results are shown in figure 6, where the blue full circles, the magenta full squares and the golden full diamonds respectively refer to the polydisperse octahedra, cubes and tetrahedra. The figure represents a first test on the reliability of approximating an exact CF by a polynomial one to perform a polydisperse analysis. It shows that the resulting $p(r)$ is reliable if the particle exact scattering intensity is reasonably approximated by the polynomial polydisperse one. It is noted that the agreement must be observed in the Porod plot of the intensities because the inversion

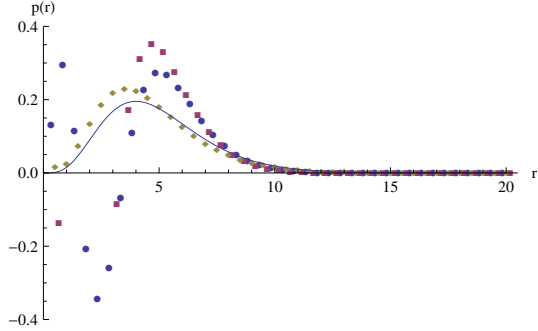


Figure 6: Reconstruction of $p(r)$ by (99) using the 'exact' scattering intensities of the polydisperse octahedrons (blue full circles), cubes (magenta full squares) and tetrahedrons (golden full diamonds). The continuous curve is the outset (4,1) Poisson distribution.

formulae involve quantity $q^4 I(q)$ in their integrands. This appears to be the case of tetrahedral particles, while the 3rd degree polynomial approximation is not equally satisfactory in the case of cubes and octahedra. In fact, one sees that the resulting $p(r)$ s are satisfactory in the only outer r -range. In the small/medium r -range they are not satisfactory because the polynomial polydisperse intensities do not accurately approximate the polydisperse exact ones in the region $q < 2$ (see figure 5B).

6.3 The 4th degree polynomial approximation

For greater completeness we shall now briefly report the results that are obtained in the cases of (4.1) Poisson distributions of tetrahedrons, octahedrons or cubes when the relevant CFs are approximated by a 4th degree polynomial $P_4(r)$. One requires that $P_4(r)$ obeys constraints $a)$, $b)$, $c)$, $d)$ and $e)$. Then one finds that

$$P_4(r) = 1 + r\sigma - \frac{5r^2(8\pi + 3\pi\sigma - 21v)}{4\pi} - \frac{r^3(-32\pi - 9\pi\sigma + 105v)}{2\pi} - \frac{7r^4(4\pi + \pi\sigma - 15v)}{4\pi}, \quad (103)$$

where v and σ respectively denote the volume and the specific surface of the considered unit polyhedron. The substitution of the σ and v relevant to the unit regular tetrahedron, octahedron and cube yields the 4th degree polynomial approximations of the respective CFs. The left panel of Figure 7 compares the exact CFs to their 4th degree approximations, while the right panel shows the exact and the approximated form factors of the three particle shapes. It is evident that the agreement is far better than in Fig. 3. The functions $G(r)$, relevant to the (4,1) Poisson polydisperse collections of tetrahedrons, octahedrons and cubes, can algebraically be evaluated by (40),

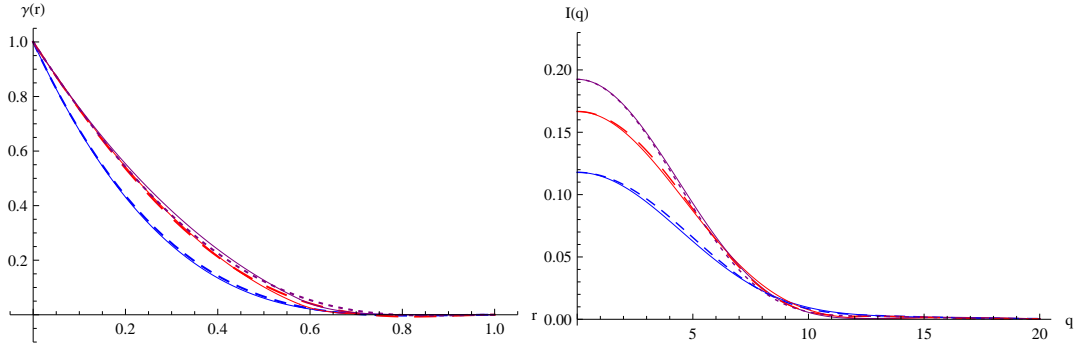


Figure 7: Left panel: The continuous and the broken curves shows the exact and the 4th degree polynomially approximated CFs of the tetrahedron (blue), octahedron (red) and cube (magenta) of unit maximal chord. Right panel: The FTs of the previous quantities are shown with the same symbols.

(38) and (103). They can also be Fourier transformed in a closed algebraic form. The results are shown in Figure 8. The comparison with the results reported in Fig. 4 shows that the 4th degree approximation is more accurate than the 3rd degree one even though some discrepancies still survive in the range $1 < q < 3$ for the octahedron and cube cases. We proceed now to

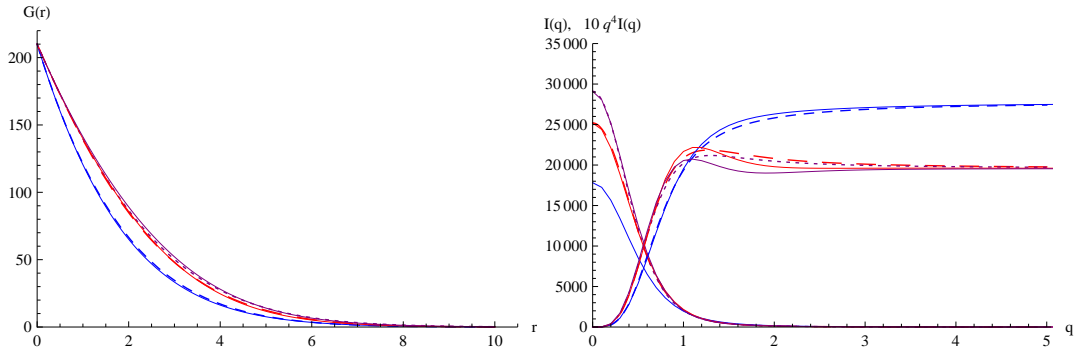


Figure 8: Left panel: The continuous and the broken curves refer to the $G(r)$ s obtained with the exact CFs and their 4th degree approximations. The blue, red and magenta curves respectively refer to the tetrahedron, octahedron and cube (4,1) Poisson collections. Right panel: behaviour of the corresponding intensities and their Porod plots.

apply the generalized Fedorova-Schmidt method. One has $M = 4$ and $m = 1$ so that $M_P = 2$. The resolvent equation (50) is a 2nd degree one that can immediately be written down because the coefficients $g_3(\sigma, v)$, $g_4(\sigma, v)$ and

$g_5(\sigma, v)$ are obtained from (103) according to definition (42). The roots are

$$\alpha_1(\sigma, v) = \frac{-\pi(64 + 15\sigma) + 105v + \Delta_4(\sigma, v)}{\pi(32 + 6\sigma) - 210v}, \quad (104)$$

$$\alpha_2(\sigma, v) = \frac{\pi(64 + 15\sigma) - 105v - \Delta_4(\sigma, v)}{\pi(32 + 6\sigma) - 210v} \quad (105)$$

with

$$\Delta_4(\sigma, v) \equiv \sqrt{\pi^2(64 + 9\sigma)^2 + 210\pi(-64 + 9\sigma)v + 11025v^2}. \quad (106)$$

Using the σ and v values of the considered three solids one finds

$$\alpha_{1,t} \approx 4.55566, \quad \alpha_{1,o} \approx 1.35395, \quad \alpha_{1,c} \approx 1.47030, \quad (107)$$

$$\alpha_{2,t} \approx -9.32024, \quad \alpha_{2,o} \approx -8.73758, \quad \alpha_{2,c} \approx -11.9556. \quad (108)$$

For the three cases, the resolvent kernels are immediately obtained from (76) recalling that $A_1(\alpha) = (\alpha_2 - \alpha_1) = -A_2(\alpha)$. They have the general form $Q_r^3 \kappa_4(Q_r)$ and $\kappa_4(Q_r)$ is a function such that its integral over the range $0 < q < Q_M$ becomes weakly equal to zero as $Q_M \rightarrow \infty$. Then the integral transforms that determine the size distributions from the observed intensities have the form of equations (90), (76), (102). Figure 9 shows the results in the cases where the scattering intensities are equal to the FTs of equation (40) with $\gamma(r)$ equal to $P_{4,t}(r)$, $P_{4,o}(r)$ and $P_{4,c}(r)$ and $\mathcal{P}(r) = r^3 p(4, 1, r)$. The agreement is as satisfactory as in the case of the 3rd degree approximation (see figure 2).

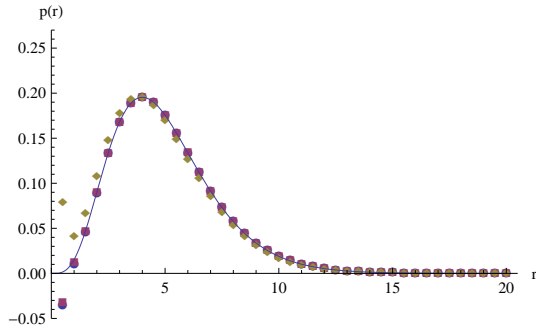


Figure 9: The continuous curve represents the (4,1) Poisson size distribution and the symbols the size distributions obtained by the generalized Fedorova-Schmidt integral equation for the 4th degree polynomial approximations of the CF of the octahedron (blue full circles), the cube (red full squares) and tetrahedron (golden full diamonds). The intensities are the (4,1) polidisperse ones evaluated with the 4th degree polynomial approximations.

Figure 10 shows the resulting size distributions in the cases where the scattering intensities are the FTs of (40) with $\gamma(r)$ equal to the exact CFs of the

considered three platonic solids. These intensities are the observable ones. Thus Figure 10 shows the accuracy that can be achieved by the 4th degree approximation of the CFs. The comparison of Fig. 10 with Fig. 6 shows the greater accuracy of the 4th degree approximation. The surviving discrepancies are not large enough to make meaningless the application of the generalized Fedorova-Schmidt method to dilute polydisperse real samples of particles with the above considered polyhedral shapes.

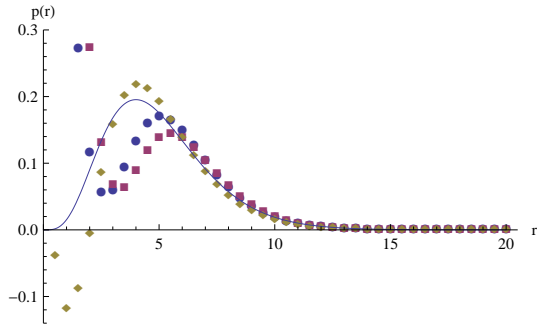


Figure 10: Reconstruction of $p(r)$ using the 'exact' scattering intensities of the polydisperse octahedrons (blue full circles), cubes (magenta full squares) and tetrahedrons (golden full diamonds) and the resolvent kernels relevant to the 4th degree polynomial approximations. The continuous curve is the outset (4,1) Poisson distribution.

7 Conclusions

The main results of this paper are: a) a reformulation of polydisperse analysis based on the stick probability functions. This presentation should have made more clear the fact that if the system is not very dilute, the polydisperse analysis is applied to an intensity that, on the average, is somewhat smaller than the exact $I_p(q)$; b) the derivation of the integral transform that determines the particle size distribution from the scattering intensity under the assumption that the particles have a polynomial CFs; c) the procedure for determining an M th degree polynomial approximation to a given CF and finally d) the application of this procedure to (4,1) Poisson distributions of cubes, octahedrons and tetrahedrons using the lowest significant polynomial approximations, i.e. the 3rd and the 4th degree ones. For the polynomial approximation to yield accurate results it is required that $q^4 I_{pol}(q)$ be fairly close to $q^4 I_{exc}(q)$, where $I_{exc}(q)$ denotes the polydisperse intensity evaluated with the particle's exact form factor and $I_{pol}(q)$ the FT of the considered polydisperse polynomial approximation.

Overall the reported results indicate that polydisperse analyses of real scattering data might be satisfactorily carried through with non spherical particles treated in the appropriate polynomial approximation.

A Derivation of equation (52)

It is now proved that function $X(r)$, defined by Equation. (52), is a solution of differential equation (46).

To this aim it is first observed that equation (46) can be written as

$$\mathcal{P}^{(M_P)}(r) + A_1(r)\mathcal{P}^{(M_P-1)}(r) + \dots + A_{M_P}(r)\mathcal{P}(r) = \frac{r^{m+1}G^{(M+1)}(r)g_{m+1}}{g_{m+1}}, \quad (109)$$

where functions $A_1(r), \dots, A_{M_P}(r)$ result from the explicit evaluation of the derivatives present in (46) and, after regrouping the terms, multiplying the results by $-r^{m+1}/g_{m+1}$. Functions $Y(r, c_1, \dots, c_{M_P})$ and $Y(r, C_1(y), \dots, C_{M_P}(y))$ also are the general integral and a particular solution of the homogenous differential equation associated to (109) because this differs from (48) by a factor.

The first derivative of $X(r)$ is easily obtained from Equation. (52) and reads

$$X'(r) = -Y(r, C_1(r), \dots, C_{M_P}(r)) \left(\frac{r^{m+1}G^{(M+1)}(r)}{g_{m+1}} \right) - \int_{r_0}^r Y'(r, C_1(y), \dots, C_{M_P}(y)) \left(\frac{y^{m+1}G^{(M+1)}(y)}{g_{m+1}} \right) dy, \quad (110)$$

where the prime denotes the derivative with respect to r . Using the first of Equation.s (53) one gets

$$X'(r) = - \int_{r_0}^r Y'(r, C_1(y), \dots, C_{M_P}(y)) \left(\frac{y^{m+1}G^{(M+1)}(y)}{g_{m+1}} \right) dy. \quad (111)$$

In a similar way, for $k = 1, \dots, (M_P - 1)$, one finds that

$$X^{(k)}(r) = - \int_{r_0}^r Y^{(k)}(r, C_1(y), \dots, C_{M_P}(y)) \left(\frac{y^{m+1}G^{(M+1)}(y)}{g_{m+1}} \right) dy. \quad (112)$$

The M_P th derivative is

$$X^{(M_P)}(r) = - \left(\frac{r^{m+1}G^{(M+1)}(r)}{g_{m+1}} \right) - \int_{r_0}^r Y^{(M_P)}(r, C_1(y), \dots, C_{M_P}(y)) \left(\frac{y^{m+1}G^{(M+1)}(y)}{g_{m+1}} \right) dy. \quad (113)$$

Thus one finds that

$$\sum_{k=0}^{M_P} A_k(r) X^{(k)}(r) = - \left(\frac{r^{m+1} G^{(M+1)}(r)}{g_{m+1}} \right) - \int_{r_0}^r \left[\sum_{k=0}^{M_P} A_k(r) Y^{(k)}(r, C_1(y), \dots, C_{M_P}(y)) \right] \left(\frac{y^{m+1} G^{(M+1)}(y)}{g_{m+1}} \right) dy. \quad (114)$$

The expression within the square brackets is equal to zero because $Y(r, C_1(y), \dots, C_{M_P}(y))$ is a solution of the homogeneous differential equation. In this way one finds that

$$\sum_{k=0}^{M_P} A_k(r) X^{(k)}(r) = - \left(\frac{r^{m+1} G^{(M+1)}(r)}{g_{m+1}} \right), \quad (115)$$

and the proof that $X(r)$ is a particular integral of Equation. (A.1) is achieved. It is now proved that (55) are the solution of Equation.s (53). To this aim one puts $f_i(r) = r^{\alpha_i}$ for i, \dots, M_P and one writes $Y(y, C_1, \dots, C_{M_P})$ as $\sum_{i=1}^{M_P} C_i f_i(y)$. Equation.s (53) become

$$\begin{aligned} \sum_{i=1}^{M_P} C_i f_i(y) &= 0, \\ \sum_{i=1}^{M_P} C_i f_i'(y) &= 0 \\ &\dots = \dots \\ \sum_{i=1}^{M_P} C_i f_i^{(M_P)}(y) &= 1. \end{aligned} \quad (116)$$

The $M_P \times (M_P + 1)$ matrix associated to this system of linear equations is

$$\begin{pmatrix} f_1 & f_2 & \dots & f_{M_P} & 0 \\ f_1' & f_2' & \dots & f_{M_P}' & 0 \\ \vdots & \vdots & \ddots & \vdots & \vdots \\ f_1^{(M_P-1)} & f_2^{(M_P-1)} & \dots & f_{M_P}^{(M_P-1)} & 1 \end{pmatrix}$$

that, using the f_i expressions, becomes

$$\begin{pmatrix} y^{\alpha_1} & y^{\alpha_2} & \dots & y^{\alpha_{M_P}} & 0 \\ \alpha_1 y^{\alpha_1-1} & \alpha_2 y^{\alpha_2-1} & \dots & \alpha_{M_P} y^{\alpha_{M_P}-1} & 0 \\ \vdots & \vdots & \ddots & \vdots & \vdots \\ (\alpha_1)_{(M_P-1)} y^{\alpha_1-M_P+1} & (\alpha_2)_{(M_P-1)} y^{\alpha_2-M_P+1} & \dots & (\alpha_{M_P})_{(M_P-1)} y^{\alpha_{M_P}-M_P+1} & 1 \end{pmatrix}. \quad (117)$$

The determinant Δ of the $(M_P \times M_P)$ matrix, formed by the first M_P columns of (117), is the determinant of the coefficients. It is simply evaluated observing that if one multiplies the terms of the k th row by y^{k-1} for $k = 1, \dots, M_P$, the j th column terms have y^{α_j} as common factor. After extracting these factors, determinant Δ reduces to to the Vendermonde determinant

$$\Delta = \left(\prod_{k=1}^{M_P} y^{1-k+\alpha_k} \right) \det \begin{vmatrix} 1 & 1 & \dots & 1 \\ \alpha_1 1 & \alpha_2 1 & \dots & \alpha_{M_P} \\ \vdots & \vdots & \ddots & \vdots \\ (\alpha_1)^{(M_P-1)} & (\alpha_2)^{(M_P-1)} & \dots & (\alpha_{M_P})^{(M_P-1)} \end{vmatrix}$$

whose value is

$$\Delta = y^{(M_P(M_P-1)/2 + \sum_{i=1}^{M_P} \alpha_i)} \prod_{1 \leq i < j \leq M_P} (\alpha_i - \alpha_j). \quad (118)$$

To get the expression of coefficient C_k one must evaluate the determinant of the $(M_P \times M_P)$ matrix obtained omitting the k th column in equation (117) and multiply the result by $1/\Delta$. The value of determinant is evaluated by the same procedure expounded above. Its value is

$$(-1)^{k-1} y^{((M_P-1)(M_P-2)/2 + \sum'_{i=1}^{M_P} \alpha_i)} \prod'_{1 \leq i < j \leq M_P} (\alpha_i - \alpha_j), \quad (119)$$

where the primes on the sum and product symbols denote that the sum and the product indices cannot be equal to k . Dividing this result by Δ and simplifying one gets

$$C_k = \frac{y^{M_P-1-\alpha_k}}{\prod'_j (\alpha_k - \alpha_j)} \quad (120)$$

that is Equation.(54).

B Derivation of equation. (77)

First of all the definition of the symbols present in Equation. (??) are as follows. The prime on the sum denotes that index l ranges over the even numbers and that h, k, l obey the constraint $h + k + l = m$;

$$\langle R^{2h} \rangle \equiv \frac{1}{V} \int r^{2h} \rho_p(\mathbf{r}) dv, \quad h = 0, 1, 2, \dots \quad (121)$$

where $\rho_p(\mathbf{r})$ is the characteristic function of the particle that has its gravity center set at the origin of the Cartesian frame and its maximal chord equal to one and,finally,

$$a_l \equiv \frac{2^l}{l+1}. \quad (122)$$

The $2m$ th moment of $\gamma(r)$, using the CF definition, can be written as

$$\begin{aligned} \mathcal{G}_{2m} &= \int r^{2m} \gamma(r) dv = \frac{1}{V} \int r^{2m} dv \int \rho_p(\mathbf{r}_2) \rho_p(\mathbf{r}_2 + \mathbf{r}) dv_2 = \\ &= \frac{1}{V} \int dv_1 \int \rho_p(\mathbf{r}_2) \rho_p(\mathbf{r}_1) (\mathbf{r}_1 - \mathbf{r}_2)^{2m} dv_2. \end{aligned} \quad (123)$$

One has

$$(\mathbf{r}_1 - \mathbf{r}_2)^{2m} = (r_1^2 - 2\mathbf{r}_1 \cdot \mathbf{r}_2 + r_2^2)^m = \sum_{0 \leq h, k, l \leq m} \frac{m! (-2)^l}{h! k! l!} r_1^{2h} r_2^{2k} (\mathbf{r}_1 \cdot \mathbf{r}_2)^l \quad (124)$$

with the further constraint $h + k + l = m$, and (123) becomes

$$\mathcal{G}_{2m} = \sum_{0 \leq h, k, l \leq m} \frac{m! (-2)^l}{h! k! l! V} \mathcal{I}_{a_1, \dots, a_l}^{2h, l} \mathcal{I}_{a_1, \dots, a_l}^{2k, l} \quad (125)$$

where it has been put

$$\mathcal{I}_{a_1, \dots, a_l}^{2h, l} \equiv \int r_1^{2h} \mathbf{r}_{1, a_1} \dots \mathbf{r}_{1, a_l} \rho_p(\mathbf{r}_1) dv_1 \quad (126)$$

and the convention of summing over repeated indices has been adopted. Quantity $\mathcal{I}_{a_1, \dots, a_l}^{2h, l}$ is a fully symmetric tensor of rank l that must behave as a scalar quantity. Hence it has the form

$$\mathcal{I}_{a_1, \dots, a_l}^{2h, l} = \mathcal{I}_0^{2h, l} \mathcal{S}_{a_1, \dots, a_l}^l \quad (127)$$

where the $\mathcal{I}_0^{2h, l}$ expressions must be determined and $\mathcal{S}_{a_1, \dots, a_l}^l$ is a fully symmetric tensor resulting from the sum of terms having the form $\delta_{a_1, a_{i_2}} \delta_{a_{i_3}, a_{i_4}} \dots \delta_{a_{i_{l-1}}, a_{i_l}}$ where $\delta_{a, b}$ is the (3×3) Kronecker symbol and i_2, i_3, \dots, i_l is a permutation of $\{2, 3, \dots, l\}$ such that $i_3 < i_4, i_5 < i_6, \dots$, and $i_{l-1} < i_l$. Clearly the existence of $\mathcal{S}_{a_1, \dots, a_l}^l$ requires that l be even. If one saturates two indices of $\mathcal{I}_{a_1, \dots, a_l}^{2h, l}$, from definition (126) one gets

$$\mathcal{I}_{a, a, a_3, \dots, a_l}^{2h, l} = \mathcal{I}_{a_3, \dots, a_l}^{2h+2, l-2} \quad (128)$$

and by (127) that

$$\mathcal{I}_0^{2h, l} \mathcal{S}_{a, a, a_3, \dots, a_l}^l = \mathcal{I}_0^{2h+2, l-2} \mathcal{S}_{a_3, \dots, a_l}^{l-2}. \quad (129)$$

Quantity $\mathcal{S}_{a, a, a_3, \dots, a_l}^l$ can be explicitly related to $\mathcal{S}_{a_3, \dots, a_l}^{l-2}$. In fact from the \mathcal{S}^l definition follows

$$\mathcal{S}_{a_1, a_2, a_3, \dots, a_l}^l = \delta_{a_1, a_2} \mathcal{S}_{a_3, \dots, a_l}^{l-2} + \sum_{3 \leq k \leq l} \delta_{a_1, a_k} \mathcal{S}_{a_2, \dots, a_l, \hat{k}}^{l-2}, \quad (130)$$

where symbol \hat{k} means that index a_k is not present. Saturating a_1 with a_2 in (130), one obtains that

$$\mathcal{S}_{a,a,a_3,\dots,a_l}^l = (3+l-2)\mathcal{S}_{a_3,\dots,a_l}^{l-2}. \quad (131)$$

By iteration of this relation one gets

$$\mathcal{S}_{a_1,a_1,a_3,a_3,a_5,\dots,a_{2L}}^{2L} = (2L+1)(2(L-1)+1)\mathcal{S}_{a_5,\dots,a_{2L}}^{2(L-2)},$$

and, since $\mathcal{S}_{a,a}^2 = 3$, one finds that

$$\mathcal{S}_{a_1,a_1,a_3,a_3,\dots,a_{2L-1},a_{2L-1}}^{2L} = \prod_{1 \leq j \leq L} (2j+1) = \frac{2^{L+1}\Gamma(L+3/2)}{\sqrt{\pi}}, \quad (132)$$

and, by (126) and (127),

$$\mathcal{I}^{2h,2L}_{a_1,\dots,a_{2L}} = \mathcal{I}_0^{2h+2L,0}\mathcal{S}_{a_1,\dots,a_{2L}}^{2L}/D(L) \quad (133)$$

with

$$D(L) \equiv \frac{2^{L+1}\Gamma(L+3/2)}{\sqrt{\pi}}. \quad (134)$$

To fully simplify the rhs of (125) one must saturate $\mathcal{I}^{2h,l}_{a,a,a_3,\dots,a_l}$ with itself. By relation (133), this amounts to evaluate $\mathcal{S}_{a_1,\dots,a_{2L}}^{2L}\mathcal{S}_{a_1,\dots,a_{2L}}^{2L}$. This quantity by (130) becomes equal to (it is recalled that $l = 2L$)

$$\begin{aligned} & 3\mathcal{S}_{a_3,\dots,a_l}^{l-2}\mathcal{S}_{a_3,\dots,a_l}^{l-2} + 2\delta_{a_1,a_2}\mathcal{S}_{a_3,\dots,a_l}^{l-2} \sum_{3 \leq k \leq l} \delta_{a_1,a_k}\mathcal{S}_{a_2,\dots,a_l,\hat{k}}^{l-2} + \\ & \sum_{3 \leq k,j \leq l} \delta_{a_1,a_k}\mathcal{S}_{a_2,\dots,a_l,\hat{k}}^{l-2}\delta_{a_1,a_j}\mathcal{S}_{a_2,\dots,a_l,\hat{j}}^{l-2}. \end{aligned} \quad (135)$$

The second term is equal to $2 \times 2(L-1)\mathcal{S}_{a_3,\dots,a_{2(L-1)}}^{2(L-1)}\mathcal{S}_{a_3,\dots,a_{2L}}^{l-2}$, while the third term can be written as

$$\begin{aligned} & \sum_{3 \leq j \leq l} \delta_{a_j,a_j}\mathcal{S}_{a_2,\dots,a_{2L},\hat{j}}^{2(L-1)}\mathcal{S}_{a_2,\dots,a_l,\hat{j}}^{2(L-1)} + \\ & \sum_{3 \leq j \neq k \leq l} \delta_{a_j,a_k}\mathcal{S}_{a_2,\dots,a_{2L},\hat{k}}^{2(L-1)}\mathcal{S}_{a_2,\dots,a_{2L},\hat{j}}^{2(L-1)} = \\ & [3 \times 2(L-1) + (2L-3)(2L-4)]\mathcal{S}_{a_3,\dots,a_{2(L-1)}}^{2(L-1)}\mathcal{S}_{a_3,\dots,a_{2L}}^{l-2} \end{aligned}$$

Collecting the above results one finds that

$$\mathcal{S}_{a_1,\dots,a_{2L}}^{2L}\mathcal{S}_{a_1,\dots,a_{2L}}^{2L} = (4L^2 - 1)\mathcal{S}_{a_3,\dots,a_{2L}}^{2(L-1)}\mathcal{S}_{a_3,\dots,a_{2L}}^{2L-2}.$$

Iterating one gets

$$\mathcal{S}_{a_1, \dots, a_{2L}}^{2L} \mathcal{S}_{a_1, \dots, a_{2L}}^{2L} = \prod_{1 \leq j \leq L} (4j^2 - 1) = \frac{2^{L+\frac{1}{2}} \Gamma(L + \frac{1}{2}) \Gamma(L + \frac{3}{2})}{\pi}. \quad (136)$$

Finally, one finds that

$$\mathcal{G}_{2m} = \sum'_{0 \leq h, k, l \leq m} \frac{m! (2)^{2L}}{h! k! l! (l+1) V} \mathcal{I}^{2h+2L, 0} \mathcal{I}^{2k+2L, 0}. \quad (137)$$

Recalling definitions (121) and (122) the proof of (77) is completed. The relation can easily be checked in the case of a spherical unit particle since by direct evaluation one finds, from Equation. (82), that

$$\mathcal{G}_{2m} = \frac{12\pi}{72 + 108m + 52m^2 + 8m^3} \quad (138)$$

and from (121) that

$$\langle R^{2h} \rangle = \frac{3 \times 2^{-2m}}{3 + 2m}. \quad (139)$$

References

- Abramowitz, M. & Stegun, I.A. (1970). *Handbook of Mathematical Functions*, New York: Dover.
- Bender, C.M. & Orszag, S. A. (1978). *Advanced Mathematical Methods for Scientists and Engineers*. New York: McGraw-Hill, §3.3 and 3.4.
- Botet, R. & Cabane, B. (2012). *J. Appl. Cryst.* **45**, 406-416.
- Ciccariello, S. (1984). *J. Appl. Phys.* **56**, 162-67.
- Ciccariello, S. (2014). *J. Appl. Cryst.* **47**, in the press; arXiv: 1407.2788v1.
- Ciccariello, S. & Sobry, R. (1995). *Acta Cryst. A* **51**, 60-69.
- Ciccariello, S., Cocco, G., Benedetti, A. & Enzo, S. (19881). *Phys. Rev.* **B23**, 6474-6485.
- Debye, P., Anderson, H.R. & Brumberger, H. (1957). *J. Appl. Phys.* **20**, 679-683.
- Fedorova, I.S. & Schmidt, P.W. (1978). *J. Appl. Cryst.* **11**, 405-11.
- Feigin, L.A. & Svergun, D.I. (1987). *Structure Analysis by Small-Angle X-Ray and Neutron Scattering*, (Plenum Press, New York).
- Gille, W. (2013). *Particle and Particle Systems characterization*, (CRC Press, London)
- Goodisman, J. (1980). *J. Appl. Cryst.* **13**, 132-34.
- Goodisman, J. & Brumberger, H. (1971). *J. Appl. Cryst.* **4**, 347-351.
- Goursat, E. (1959). *Differential Equations*. New York: Dover, § 38 and 39.
- Guinier, A. (1946). *Compt. Rend.* **223**, 161-162.
- Guinier, A. & Fournet, G. (1955). *Small-Angle Scattering of X-rays*. New York: John Wiley.
- Kirste, R. & Porod, G. (1962). *Kolloid Z.* **184**, 1-6.
- Letcher, J.H. & Schmidt, P.W. (1966). *J. Appl. Phys.* **37**, 649-655.
- Luke, Y.L. (1969). *The Special Functions and Their Approximations*, Vol. I, Academic Press:New York.
- Méring, J. & Tchoubar, D. (1968). *J. Appl. Cryst.* **1**, 153-65.
- Moore, P.B. (1980). *J. Appl. Cryst.* **13**, 168-175.
- Pedersen, J.S. (1994). *J. Appl. Cryst.* **27**, 595-608.

Porod, G. (1951). *Kolloid Z.* **124**, 83-114.

Porod, G. (1967). *Small-Angle X-Ray Scattering. Proceedings of the Syracuse Conference*, edited by H. Brumberger, 1-8, Gordon & Breach:New York.

Roess, L.C. (1946). *J. Chem. Phys.* **14**, 695-697.

Roess, L.C. & Shull, C.G. (1947). *J. Appl. Phys.* **18**, 308-313.

Taupin, D. & Luzzatti, V. (1982). *J. Appl. Cryst.* **15**, 289-300.